Theory of optical scintillation: Gaussian-beam wave model

Ammar Al-Habash, Larry Andrews, R. Phillips

Ammar Al-Habash, Larry C. Andrews, R. L. Phillips, "Theory of optical scintillation: Gaussian-beam wave model," Proc. SPIE 4678, Eighth International Symposium on Atmospheric and Ocean Optics: Atmospheric Physics, (28 February 2002); doi: 10.1117/12.458427

SPIE.

Event: Eighth Joint International Symposium on Atmospheric and Ocean Optics: Atmospheric Physics, 2001, Irkutsk, Russian Federation

Theory of Optical Scintillation: Gaussian-Beam Wave Model

M. A. Al-Habash
TeraBeam Networks
Redmond, WA 98052

L. C. Andrews
Department of Mathematics and
School of Optics/CREOL
University of Central Florida, Orlando, FL 32816

R. L. Phillips
Director of Florida Space Institute (FSI) and
Department of Electrical and Computer Engineering
University of Central Florida, Orlando, FL 32816

ABSTRACT

Under the assumption that small-scale irradiance fluctuations are modulated by large-scale irradiance fluctuations, we develope a heuristic model of irradiance fluctuations for a propagating optical wave in a weakly inhomogeneous medium. This model takes into account the loss of spatial coherence as the optical wave propagates through atmospheric turbulence by eliminating effects of certain turbulent scale sizes that exist between two scale size, hereafter called the upper bound and the lower bound. These mid-range scale size effects are eliminated through the formal introduction of spatial frequency filters that continually adjust spatial cutoff frequencies as the optical wave propagates. By applying a modification of the Rytov method that incorporates an amplitude spatial frequency filter function under strong fluctuation conditions, tractable expressions are developed for the scintillation index of a Gaussian beam wave that are valid under moderate-to-strong irradiance fluctuations. Inner scale effects are taken into account by use of a modified atmospheric spectrum that exhibits a "bump" at large spatial frequencies. We also include the effect of a finite outer scale in addition to inner scale. With a finite outer scale, the scintillation index can be substantially lower in strong turbulence than that predicted by a model with an infinite outer scale. Based on this doubly stochastic theory of scintillation we also develop a probability density function (PDF) for the irradiance fluctuation of and optical wave propagation through a turbulent medium. The resulting irradiance PDF takes the form of a generalized K distribution which we call the gamma-gamma distribution. The two parameters of this PDF are determined from the large-scale and small-scale scintillation terms above. We make a number of comparisons of the gamma-gamma PDF with published plane wave and spherical wave simulation data.

Keywords: Optical Scintillation, Irradiance Probability Density Function, moderate and strong turbulence.

2. THE GAUSSIAN BEAM PARAMETERS

In the transverse plane of the exit aperture of the transmitter a unit amplitude Gaussian-beam wave model is described by

$$U_0(\mathbf{r},0) = \exp\left(-\frac{r^2}{W_0^2} - \frac{ikr^2}{2F_0}\right), \tag{1}$$

where $\mathbf{r}$ is a transverse vector, $i = \sqrt{-1}$, W_0 is the beam radius, and F_0 is the phase front radius of curvature. For a receiver at distance L from the input plane, under the paraxial approximation, the free-space Gaussian-beam wave assumes the form [1,2]

Eighth International Symposium on Atmospheric and Ocean Optics,
Gelii A. Zherebtsov, Gennaddi G. Matvienko Victor A. Banakh, Vladimir V. Koshelev, Editors,
Proceedings of SPIE Vol. 4678 (2002) © 2002 SPIE · 0277-786X/02/$15.00

$$U_0(\mathbf{r},L) = \frac{1}{\Theta_0 + i\Lambda_0}\exp\left(ikL - \frac{r^2}{W^2} - i\frac{kr^2}{2F}\right), \tag{2}$$

where

$$\Theta_0 = 1 - \frac{L}{F_0}, \quad \Lambda_0 = \frac{2L}{kW_0^2}, \quad W = W_0(\Theta_0^2 + \Lambda_0^2)^{1/2}, \tag{3}$$

and where W and F represent the beam radius and phase front radius of curvature, respectively, at the receiver. These beam characteristics in the receiver plane are related to the beam parameters (3) according to

$$F = \frac{F_0(\Theta_0^2 + \Lambda_0^2)(\Theta_0 - 1)}{\Theta_0^2 + \Lambda_0^2 - \Theta_0}. \tag{4}$$

Based on these beam characteristics, the log-irradiance variance of a Gaussian-beam wave under weak fluctuation theory takes the form [1,3]

$$\begin{aligned}\sigma_{\ln I}^2(\mathbf{r},L) &= 8\pi^2k^2L\int_0^1\int_0^\infty \kappa\Phi_n(\kappa)\exp\left(-\frac{\Lambda L\kappa^2\xi^2}{k}\right)\times\left\{I_0(2\Lambda r\kappa\xi) - \cos\left[\frac{L\kappa^2}{k}\xi(1-\bar{\Theta}\xi)\right]\right\}d\kappa\,d\xi \\ &= \sigma_{\ln I,r}^2(\mathbf{r},L) + \sigma_{\ln I,l}^2(L),\end{aligned} \tag{5}$$

where

$$\sigma_{\ln I,r}^2(\mathbf{r},L) = 8\pi^2k^2L\int_0^1\int_0^\infty \kappa\Phi_n(\kappa)\exp\left(-\frac{\Lambda L\kappa^2\xi^2}{k}\right)\times\left[I_0(2\Lambda r\kappa\xi) - 1\right]d\kappa\,d\xi, \tag{6}$$

$$\sigma_{\ln I,l}^2(L) = 8\pi^2k^2L\int_0^1\int_0^\infty \kappa\Phi_n(\kappa)\exp\left(-\frac{\Lambda L\kappa^2\xi^2}{k}\right)\times\left\{1 - \cos\left[\frac{L\kappa^2}{k}\xi(1-\bar{\Theta}\xi)\right]\right\}d\kappa\,d\xi. \tag{7}$$

The first term (6) is the radial component and the second term (7) is the longitudinal component, the latter of which is independent of position in the beam. Here, $I_0(x)$ is a modified Bessel function, $\Phi_n(\kappa)$ is the spatial power spectrum of refractive-index fluctuations, and Θ and Λ are receiver plane beam parameters defined by

$$\Theta = \frac{\Theta_0}{\Theta_0^2 + \Lambda_0^2} = 1 + \frac{L}{F}, \qquad \bar{\Theta} = 1 - \Theta, \qquad \Lambda = \frac{\Lambda_0}{\Theta_0^2 + \Lambda_0^2} = \frac{2L}{kW^2}. \tag{8}$$

The parameter Θ describes amplitude change in the wave caused by focusing (refraction) and Λ describes amplitude change caused by diffraction.

Because of diffraction effects, the spot size and phase front radius of curvature of a Gaussian beam continually change as the beam propagates through a vacuum. In the presence of optical turbulence, additional diffraction and refraction cause further broadening of the beam spot size and further focusing and defocusing, the latter attributed to changes in the phase front radius of curvature [4-8]. These additional diffraction and refraction effects define an effective spot radius and effective phase front radius of curvature of the beam that are given by

$$W_e = W\left(1 + 1.625\sigma_1^{12/5}\Lambda\right)^{1/2}, \qquad F_e = -\frac{L(1 + 1.625\sigma_1^{12/5}\Lambda)}{\bar{\Theta} + 2.438\sigma_1^{12/5}\Lambda}. \tag{9}$$

The Rytov variance is defined as

$$\sigma_1^2 = 1.23 C_n^2 k^{7/6} L^{11/6}, \tag{10}$$

where C_n^2 is the index of refraction structure parameter, k is the optical wave number, and L is the propagation path length between transmitter and receiver. The Rytov variance represents the scintillation index of an unbounded plane wave in weak fluctuations, but is otherwise considered a measure of optical turbulence strength when extended to strong fluctuation regimes by increasing either C_n^2 or the path length L, or both.
It has been shown that the use of effective beam parameters permits us to formally extend weak fluctuation expressions for the spatial coherence radius into the strong fluctuation regime [6,7]. A similar observation was made by Miller et al. [4] in extending weak fluctuation scintillation expressions further into the focusing regime. This is accomplished in a heuristic manner by simply replacing the receiver beam parameters Θ and Λ with the effective beam parameters

$$\Lambda_e = \frac{2L}{kW_e^2} = \frac{\Lambda}{1 + 1.625\sigma_1^{12/5}\Lambda}. \tag{11}$$

$$\Theta_e = 1 + \frac{L}{F_e} = \frac{\Theta - 0.813\sigma_1^{12/5}\Lambda}{1 + 1.625\sigma_1^{12/5}\Lambda}, \qquad \bar{\Theta}_e = 1 - \Theta_e, \tag{12}$$

Note that in weak fluctuation regimes ($\sigma_1^2 \ll 1$), the effective beam parameters (13) and (14) reduce to the free-space parameters Θ and Λ.

3. REVIEW OF SCINTILLATION THEORY

In the approach utilized here to develop tractable scintillation models under general fluctuation conditions, we start with the following observations and/or assumptions:

1. The received irradiance of an optical wave can be modeled as a modulation process in which small-scale (diffractive) fluctuations are multiplicatively modulated by large-scale (refractive) fluctuations.
2. Small-scale processes and large-scale processes are statistically independent.
3. The Rytov method for optical scintillation is valid even into the saturation regime with the introduction of a spatial frequency filter to properly account for the loss of spatial coherence of the optical wave in strong fluctuation regimes.
4. The geometrical optics method can be applied to large-scale irradiance fluctuations.

To model the modulation process described above, we write the normalized irradiance as $I = xy$, where x arises from large-scale turbulent eddies and y from statistically independent small-scale eddies. In this case the scintillation index is defined by [9,10]

$$\sigma_I^2 = \langle x^2 \rangle \langle y^2 \rangle - 1 = \sigma_x^2 + \sigma_y^2 + \sigma_x^2 \sigma_y^2, \tag{13}$$

where σ_x^2 and σ_y^2 are normalized variances of the large-scale and small-scale irradiance fluctuations and $\langle\ \rangle$ denotes an ensemble average. We can further express the normalized variances σ_x^2 and σ_y^2 in the form $\sigma_x^2 = \exp(\sigma_{\ln x}^2) - 1$ and $\sigma_y^2 = \exp(\sigma_{\ln y}^2) - 1$, which permits us to rewrite (13) as

$$\sigma_I^2 = \exp\left(\sigma_{\ln x}^2 + \sigma_{\ln y}^2\right) - 1, \tag{14}$$

where $\sigma_{\ln x}^2$ and $\sigma_{\ln y}^2$ are large-scale and small-scale log-irradiance variances, respectively.

In determining the log-irradiance variances appearing in (14), we treat the atmosphere like a linear spatial filter that accounts for the loss of transverse spatial coherence of the propagating wave by eliminating the effects of scale sizes between those defined by the spatial coherence radius and the scattering disk, the latter being defined by the refractive cell size l at which the focusing angle $\theta_F \sim l/L$ is equal to the average diffraction angle $\theta_D \sim 1/k\rho_0$, where ρ_0 is the spatial coherence radius of a plane wave. Under weak fluctuations it is widely accepted that the scintillation index of a plane wave or spherical wave is not greatly influenced by the outer scale of turbulence L_0, i.e., weak turbulence scintillation is primarily a small-scale effect. For example, Miller et al. [3] have shown that outer scale had no noticeable effect on scintillation near the center of the beam, similar to the limiting case of a plane wave or spherical wave. However, it was found that a finite outer scale on the order of 1-2 meters could lead to a small reduction in scintillation away from the center of the beam near the diffractive beam edge, particularly for beams with transmitter diameter ranging anywhere from 1/10 to 10 times the size of the first Fresnel zone. A filter function that eliminate the intermediate size eddies and takes into consideration the outer scale effects is formally introduced by expressing the effective spatial power spectrum of refractive-index fluctuations as

$$\Phi_{n,e}(\kappa) = 0.033\, C_n^2 \kappa^{-11/3}\left[G_x(\kappa,l_0,\kappa,L_0) + G_y(\kappa,z)\right]. \tag{15}$$

where

$$G_x(\kappa l_0,\kappa L_0) = f(\kappa l_0)\left[\exp\left(-\frac{\kappa^2}{\kappa_x^2}\right) - \exp\left(-\frac{\kappa^2}{\kappa_{x0}^2}\right)\right], \tag{16}$$

where κ_x is the lowpass cutoff spatial frequency and $\kappa_{x0}^2 = \kappa_x^2\kappa_0^2/(\kappa_x^2 + \kappa_0^2)$. For tractability reason we set $\kappa_0 = 8\pi/L_0$ and $\kappa_{x0}^2 = \kappa_x^2\kappa_0^2/(\kappa_x^2 + \kappa_0^2)$. Similarly, $G_y(\kappa,z)$ is the small-scale, or high pass, portion of the filter defined by

$$G_y(\kappa,z) = \frac{\kappa^{11/3} h(z)}{(\kappa^2 + \kappa_y^2)^{11/6}}, \tag{17}$$

where κ_y is the high pass (small-scale) spatial frequency cutoff and $h(z)$ represents a refinement in the small-scale filter function previously used for plane wave and spherical wave models that takes into account the diminishing effect of the finite beam size as a function of propagation distance z. Although small-scale scintillation in general depends on the inner scale, particularly in weak fluctuations, the inner scale effects in the small-scale scintillation will tend to diminish under strong fluctuation conditions when the coherence radius of the optical wave is smaller than the inner scale (see Ref. [9] for further details). Hence, it follows that the large-scale scintillation in this case can be expressed as the difference

$$\sigma_{\ln x}^2(l_0,L_0) = \sigma_{\ln x}^2(l_0) - \sigma_{\ln x}^2(L_0), \tag{18}$$

where $\sigma_{\ln x}^2(l_0)$ is given by

$$\sigma_{\ln x}^2(l_0) = 0.49\sigma_1^2\left(\frac{1}{3} - \frac{1}{2}\bar{\Theta} + \frac{1}{5}\bar{\Theta}^2\right)\left(\frac{\eta_x Q_l}{\eta_x + Q_l}\right)^{7/6} \times\left[1 + 1.75\left(\frac{\eta_x}{\eta_x + Q_l}\right)^{1/2} - 0.25\left(\frac{\eta_x}{\eta_x + Q_l}\right)^{7/12}\right], \tag{19}$$

and

$$\frac{1}{\eta_x} = \frac{0.38}{1 - 3.21\bar{\Theta} + 5.29\bar{\Theta}^2} + 0.47\sigma_1^2 Q_l^{1/6}\left(\frac{\frac{1}{3} - \frac{1}{2}\bar{\Theta} + \frac{1}{5}\bar{\Theta}^2}{1 + 2.20\bar{\Theta}}\right)^{6/7}. \tag{20}$$

Also by analogy,

$$\sigma_{\ln x}^2(L_0) = 0.49\sigma_1^2\left(\frac{1}{3} - \frac{1}{2}\bar{\Theta} + \frac{1}{5}\bar{\Theta}^2\right)\left(\frac{\eta_{x0}Q_l}{\eta_{x0}+Q_l}\right)^{7/6}\times\left[1 + 1.75\left(\frac{\eta_{x0}}{\eta_{x0}+Q_l}\right)^{1/2} - 0.25\left(\frac{\eta_{x0}}{\eta_0 x+Q_l}\right)^{7/12}\right]. \quad (21)$$

where $\eta_{x0} = L\kappa_{x0}^2/k = \eta_x Q_0/(\eta_x + Q_0)$ and $Q_0 = 64\pi^2 L/kL_0^2$. It is also shown that the small-scale log-irradiance variance yields

$$\sigma_{\ln y}^2(l_0) = 1.27\sigma_1^2\eta_y^{-5/6}, \quad (22)$$

where the small-scale parameter takes a form similar to the zero inner scale case, viz.,

$$\eta_y = 3(\sigma_1/\sigma_G)^{12/5}\left(1 + 0.69\sigma_G^{12/5}\right), \quad (23)$$

and where σ_G^2 is the weak fluctuations scintillation index and can be approximated the expression [1,3]

$$\sigma_G^2 = 3.86\sigma_1^2\left\{0.40\frac{[(1+2\Theta)^2+(2\Lambda+3/Q_l)^2]^{11/12}}{[(1+2\Theta)^2+4\Lambda^2]^{1/2}}\left[\frac{2.610}{[(1+2\Theta)^2Q_l^2+(3+2\Lambda Q_l)^2]^{1/4}}\sin\left(\frac{4}{3}\varphi_2+\varphi_1\right)\right.\right.$$

$$\left.\left. - \frac{0.518}{[(1+2\Theta)^2Q_l^2+(3+2\Lambda Q_l)^2]^{7/24}}\sin\left(\frac{5}{4}\varphi_2+\varphi_1\right)+\sin\left(\frac{11}{6}\varphi_2+\varphi_1\right)\right]\right.$$

$$\left. - \frac{13.401\Lambda}{Q_l^{11/6}[(1+2\Theta)^2+4\Lambda^2]} - \frac{11}{6}\left[\left(\frac{1+0.31\Lambda Q_l}{Q_l}\right)^{5/6} + \frac{1.096(1+0.27\Lambda Q_l)^{1/3}}{Q_l^{5/6}} - \frac{0.186(1+0.24\Lambda Q_l)^{1/4}}{Q_l^{5/6}}\right]\right\}, \quad (24)$$

where $Q_l = 10.89L/kl_0^2$ and

$$\varphi_1 = \tan^{-1}\left(\frac{2\Lambda}{1+2\Theta}\right), \quad \varphi_2 = \tan^{-1}\left[\frac{(1+2\Theta)Q_l}{3+2\Lambda Q_l}\right]. \quad (25)$$

Hence, Eq. (19) can be written as

$$\sigma_{\ln y}^2(l_0) = \frac{0.51\sigma_G^2}{\left(1 + 0.69\sigma_G^{12/5}\right)^{5/6}}. \quad (26)$$

Hence, the scintillation index of a Gaussian-beam wave, including inner scale, outer scale, and the radial component investigated by Miller et al. [3], is approximated by

$$\sigma_I^2(\mathbf{r},L) = 4.42\,\sigma_1^2\Lambda_e^{5/6}\left[1 - 1.15\left(\frac{\Lambda_e L}{kL_0^2}\right)^{1/6}\right]\frac{r^2}{W_e^2} + \exp\left[\sigma_{\ln x}^2(l_0) - \sigma_{\ln x}^2(L_0) + \frac{0.51\,\sigma_G^2}{\left(1 + 0.69\,\sigma_G^{12/5}\right)^{5/6}}\right] - 1. \quad \textbf{(27)}$$

The consequence of a finite outer scale on the longitudinal component of a propagating Gaussian-beam wave is illustrated by the dashed lines in Fig. 1 using Eq. (27) with $r = 0$, $L_0 = 1$ m, and inner scale values $l_0 = 2$ mm and $l_0 = 8$ mm. Also shown in Fig. 1 by the solid lines are scintillation values predicted by Eq. (27) with $L_0 = \infty$. From the figure it appears that the outer scale has negligible effect on scintillation under weak fluctuations, but for $\sigma_1 > 4$ it initially reduces scintillation toward its limiting value of unity at a steeper rate than with an infinite outer scale. For smaller values of outer scale, the effect is even more pronounced. We will examine the outer scale effect on scintillation in more detail below where we compare our theoretical model with experimental and simulation data.

4. COMPARISON WITH EXPERIMENTAL DATA

In 1993, Consortini, et al. [11] published extensive results of simultaneous measurements of irradiance fluctuations (scintillation), inner scale, and refractive-index structure parameter associated with a spherical wave propagating through homogeneous turbulence along a horizontal 1200-m path. Measured values of C_n^2 varied from 10^{-15} to 10^{-12} $m^{-2/3}$ and inner scale ranged from around 2.5 mm to 12 mm. The transmitter was an argon-ion laser operating at 0.488 μm and the diverged beam was directed into the atmosphere at a height of approximately 1.2 m above the ground. Although there is considerable scatter in the strong scintillation data in both figures, the theoretical curves taken ignoring the outer scale, i.e. $L_0 = \infty$, do pass through the middle portion of the data up to $\beta \sim 4$. For $\beta_0 > 4$ these curves generally lie above the data. Also shown in Fig. 2 by the dashed lines are theoretical values generated from Eq. (27) by letting $\Theta = \Lambda = 0$ and setting outer scale $L_0 = 0.6$ m, corresponding to half the height of the laser source above ground. Here we see the impact of outer scale for strong fluctuations characterized by $\beta_0 > 4$.

5. COMPARISON WITH SIMULATION DATA

Belmonte [12] used numerical simulation for the propagation of a collimated Gaussian-beam wave through homogeneous and isotropic turbulence that led to numerical data for a variety of statistical quantities, including the scintillation index. On-axis and off-axis scintillation were treated separately so that the contribution of radial and longitudinal components could be isolated. In Belmonte's analysis a modified von Kármán spectrum described by

$$\Phi_n(\kappa) = 0.033\,C_n^2\frac{\exp\left[-(\kappa l_0/2\pi)^2\right]}{\left(\kappa^2 + 1/L_0^2\right)^{11/6}} \quad \textbf{(28)}$$

was used to model the refractive-index fluctuations. The outer scale was 3 m, equal to the size of the numerical grid. In Fig. 3.a we replot data taken from Fig. 17 in Ref. 12 for the longitudinal, or on-axis, component of a Gaussian-beam wave scintillation index vs. radial distance *s*caled by the effective beam radius. The open circles represent simulation data and the theoretical curves come from the radial component (24).

The structure parameter was assumed constant at $C_n^2 = 10^{-12}$ $m^{-2/3}$, outer scale $L_0 = 3$ m, and the inner scale was $l_0 = 1$ cm. The optical wavelength was $\lambda = 2\,\mu$m and the beam radius at the transmitter was 7 cm. In Fig. 3.b we replot data from Fig. 21 in Ref. 12 for the radial component $\sigma_{I,r}^2(\mathbf{r},L)$ as a function of radial distance scaled by the effective beam radius. In this figure the distance is fixed at 3 km and the structure constant is . Because the theoretical model (62) is restricted to $r/W_e < 1$, we show only that portion of the curve. In general the theoretical curve with $L_0 = \infty$ (dashed line) follows the data but lies somewhat above it. However, for $L_0 = 3$ m the theoretical curve (solid line) more closely follow the data. In general, we found that the radial component is sensitive to even fairly large outer scale values like 10 m, in contrast with the behavior of the on-axis or longitudinal component to outer scale.

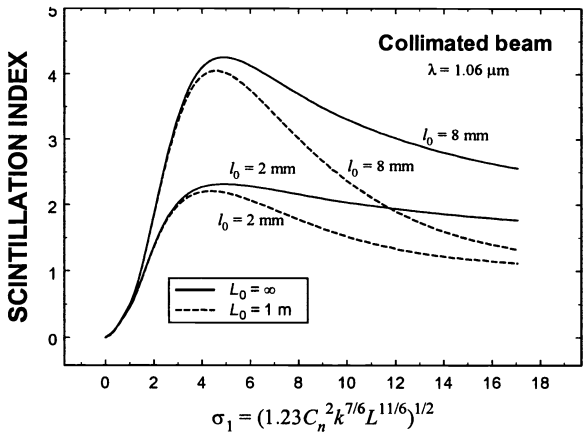

Figure 1 Gaussian-beam wave scintillation index vs. σ_1 for infinite outer scale (solid lines) and outer scale 1 m (dashed lines). Inner scale values of 2 mm and 8 mm are included in each case.

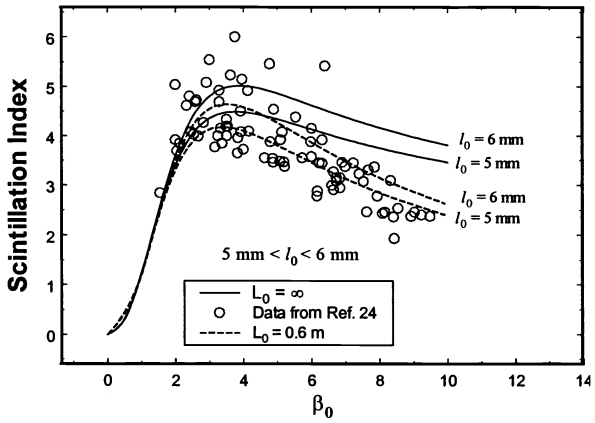

Figure 2 Open circles represent scintillation data for a fixed propagation distance of 1200 m taken from Ref. 11 and replotted here for inner scale values ranging in size between 5 and 6 mm. Solid curves are based on the scintillation theory leading to Eq. (16) with $L_0 = \infty$ and the dashed curves represent the outer scale model (27) with $L_0 = 0.6$ m.

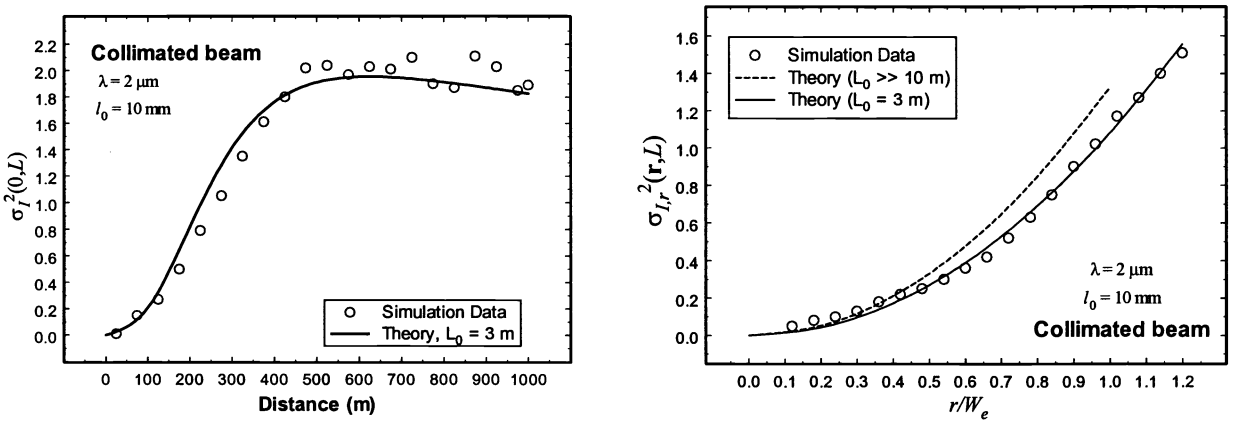

Figure 3 a. (left) On-axis Gaussian-beam wave scintillation index vs. propagation distance. The open circles represent simulation data and the solid line comes from Eq. (27) with $r = 0$. **b.** (right) Off-axis component of Gaussian-beam

6. THE PDF MODEL

To develop a PDF model of the irradiance consistent with the above theory, we make the assumption that both large-scale and small-scale irradiance fluctuations are governed by gamma distributions. This leads to the unconditional irradiance distribution:

$$p(I) = \frac{2(\alpha\beta)^{(\alpha+\beta)/2}}{\Gamma(\alpha)\Gamma(\beta)} I^{(\alpha+\beta)/2-1} K_{\alpha-\beta}\left(2\sqrt{\alpha\beta I}\right), \quad I > 0. \tag{29}$$

We call Eq. (29) the gamma-gamma distribution. The positive parameter α represents the effective number of large scale cells of the scattering process and β similarly represents the effective number of small scale cells. When optical turbulence is weak, the effective number of scale sizes smaller and larger than the first Fresnel zone is large, resulting in $\alpha \gg 1$ and $\beta \gg 1$. As the irradiance fluctuations increase and the focusing regime is approached, both parameters of (29) decrease substantially. Beyond the focusing regime and approaching the saturation regime, we find that $\beta \to 1$, indicating that the effective number of small scale cells ultimately reduces to one, determined by the transverse spatial coherence radius of the optical wave. On the other hand, the effective number of discrete refractive scatterers α increases again with increasing turbulence strength and eventually becomes unbounded in the saturation regime. Under these conditions, the gamma-gamma distribution approaches the negative exponential distribution in the deep saturation regime.

From the gamma-gamma PDF (29) we find $\langle I^2 \rangle = (1 + 1/\alpha)(1 + 1/\beta)$, and thus we identify the parameters of this distribution with the large-scale and small-scale scintillation according to

$$\alpha = \frac{1}{\sigma_x^2}, \quad \beta = \frac{1}{\sigma_y^2}. \tag{30}$$

It follows that the total scintillation index (13) is related to these parameters by

$$\sigma_I^2 = \frac{1}{\alpha} + \frac{1}{\beta} + \frac{1}{\alpha\beta}. \tag{31}$$

7. COMPARISON WITH PLANE WAVE DATA

In this section we compare the gamma-gamma distribution model with published numerical simulation data for the PDF associated with a plane wave ($\Theta = 1$, $\Lambda = 0$) [13]. The simulation data for a plane wave incident on a random medium characterized by homogeneous, isotropic Kolmogorov turbulence led to numerous plots of the log-irradiance PDF as a function of $(\ln I - \langle \ln I \rangle)/\sigma$, covering a range of conditions that extends from weak irradiance fluctuations well into the saturation regime characterized by $\sigma_1^2 = 25$. Here, $\langle \ln I \rangle$ is the mean value of the log-irradiance and $\sigma = \sqrt{\sigma_{\ln I}^2}$, the latter being the rms value of $\ln I$. The simulation PDFs were displayed in this fashion in the hope that it would reveal their salient features. In the saturation regime the simulation data of Flatté et al [13]. showed that the plane wave PDF lies somewhere between the lognormal and exponential distributions, and their moments lie between those of a lognormal-exponential distribution and those of a K distribution.

The selection of parameters based on Eq. (30) is equivalent to using only measured values of the refractive index structure parameter C_n^2 and inner scale l_0 to predict all other parameters arising in scaling the plots of the simulation data. To test the gamma-gamma model under a variety of inner scale conditions, we considered two cases presented in Fig. 7 of Ref. 3. In Fig. 4.a we use the simulation values $\sigma_1^2 = 25$, $l_0 = 0$, to predict the parameters α and β of the gamma-gamma PDF. This value of the Rytov variance corresponds to the saturation regime, in which our model predicts a scintillation index of $\sigma_{I,\mathrm{pl}}^2 = 1.214$ as compared with the higher simulation value $\sigma_{I,\mathrm{pl}}^2 = 1.387$. We also plot the K distribution using the simulation data for identifying its free parameter. In this case both distributions provide an excellent fit to the simulation data.

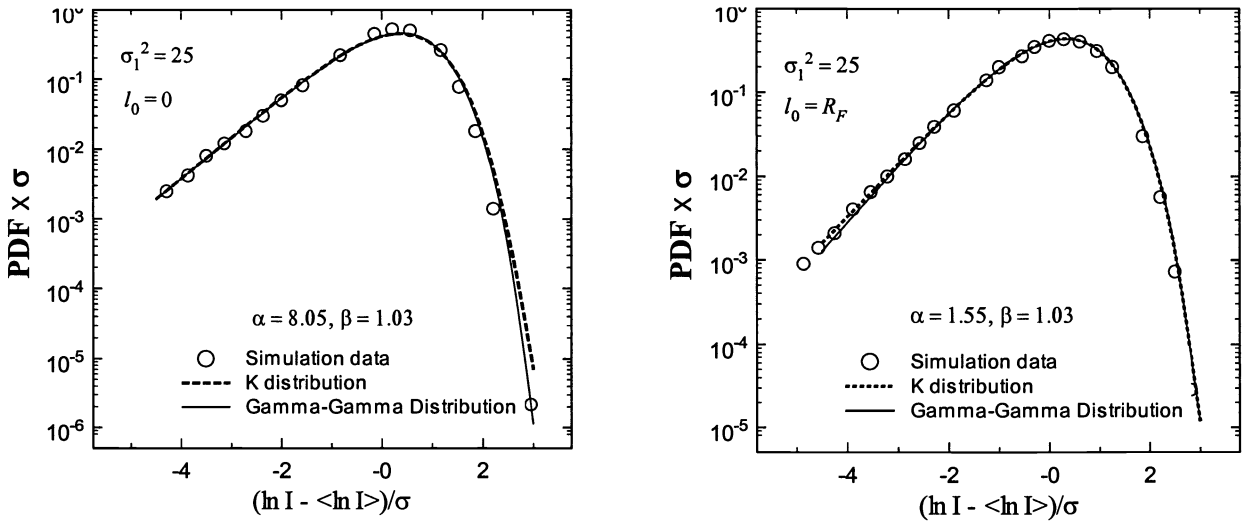

Figure 4 a. (left) PDF of the scaled log-irradiance for a plane wave in the case of strong irradiance fluctuations: $\sigma_1^2 = 25$ and $l_0/R_F = 0$. **b.** (right) Same as a. with $l_0/R_F = 1$.

In Figs 4.b we use the simulation parameter values $\sigma_1^2 = 25$, $l_0 = R_F$ ($\eta_l = 11$),b which correspond to the saturation regime but now with inner scale effects. The predicted scintillation index is found to be $\sigma_{I,\mathrm{pl}}^2 = 2.246$, whereas the simulation values are somewhat lower, viz., $\sigma_{I,\mathrm{pl}}^2 = 1.841$. However, once again both the gamma-gamma and K distributions show excellent fits with the PDF simulation data. We do note that in Figs. 4.a and 4.b the gamma-gamma parameter $\beta \cong 1$, which means there is little difference between the gamma-gamma PDF and the K distribution in this regime.

8. COMPARISON WITH SPHERICAL WAVE DATA

Hill et al. [17,18] used numerical simulation of the propagation of a spherical wave through homogeneous and isotropic atmospheric turbulence that also led to PDF data for the log-irradiance fluctuations. In that analysis they compared several heuristic PDF models with the numerical data and concluded that the Beckmann distribution provided the closest fit over all conditions tested. On the other hand, their simulation data did not generally support the K distribution.

Parameters of the gamma-gamma PDF are readily deduced from (30) and the total scintillation index is once again obtained from (14). Following Refs. 17 and 19, we plot in Figs. 5-10 simulation PDF data and PDF values predicted by the Beckmann distribution (dotted line) as a function of $(\ln I + 0.5\sigma^2)/\sigma$ and $\sigma_{\mathrm{Rytov}}^2 = 0.06$, 2, and 5. Values of r and σ_z^2 required by the Beckmann PDF (5) were provided in tabular form in Ref. 4 for various values of l_0/R_F and Rytov parameter $\sigma_{\mathrm{Rytov}}^2$. Also shown in Figs. 5-10 are curves deduced from the gamma-gamma distribution (solid line).

In Figs. 5-7, the inner scale is negligibly small. The gamma-gamma PDF curves in Figs. 5 and 7 provide very good fits with the data, but fairly large deviations in the scaled PDF can be seen in Fig. 6 for values along the left side of the abscissa (i.e., small irradiance values). We found that by incrementing the parameters α and β of the gamma-gamma PDF we could produce a "best fit" curve (dashed line) that is comparable to the fit of Beckmann's PDF. This suggests that the gamma-gamma PDF is applicable here, but the scintillation theory [14-16] used to predict α and β apparently underestimates both large-scale and small-scale scintillations in this case.

The curves and data in Figs. 8-10 are similar to that in Figs. 8 and 10 except that $l_0/R_F = 1$ ($\eta_l = 11$) in Figs. 8-10. For the case of $\sigma_{\mathrm{Rytov}}^2 = 5$ in Fig. 10, the Beckmann PDF did not lend itself directly to numerical calculations and so is omitted [13]. With the exception of Fig. 10, we believe the gamma-gamma PDF once again shows good agreement with the data. In the exceptional case we incremented the parameters of the gamma-gamma PDF as in Fig. 6 to obtain the best fit curve shown in Fig. 10 (dashed line).

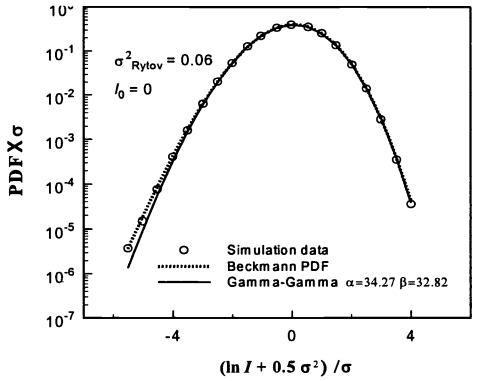

Fig. 5 PDF of the scaled log-irradiance for a spherical wave in the case of weak irradiance fluctuations: σ^2_{Rytov} = 0.06 and l_0/R_F = 0.

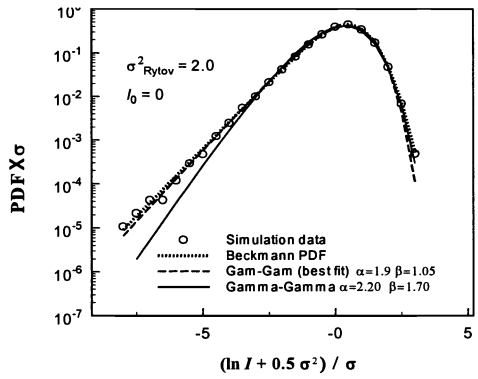

Fig. 6 Same as Fig. 5 with σ^2_{Rytov} = 2 corresponding to moderate irradiance fluctuations. Also shown (dashed line) is the gamma-gamma PDF with parameters α and β chosen from a best fit to the data

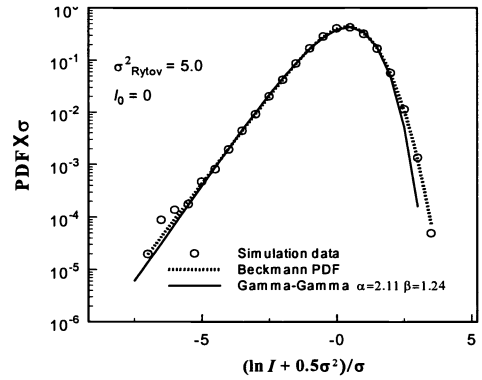

Fig. 7 Same as Fig. 5 with σ^2_{Rytov} = 5 corresponding to strong irradiance fluctuations.

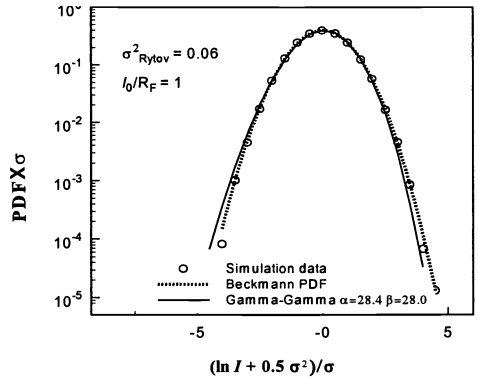

Fig. 8 Same as Fig. 5 with l_0/R_F = 1.

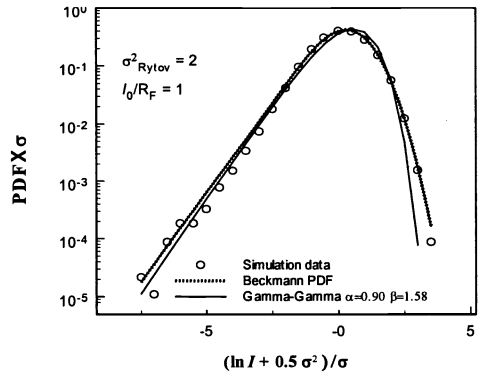

Fig. 9 Same as Fig. 8 with σ^2_{Rytov} = 2 corresponding to moderate irradiance fluctuations.

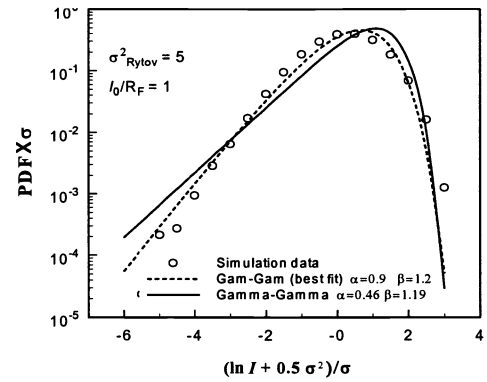

Fig. 10 Same as Fig. 8 with σ^2_{Rytov} = 5 corresponding to strong irradiance fluctuations but without the Beckmann PDF. Also shown (dashed line) is the gamma-gamma PDF with parameters α and β chosen from a best fit to the data.

ACKNOWLEDGMENT

We wish to thank Aniceto. Belmonte for providing the simulation data shown in Figs. 3.a and 3.b.

REFERENCES

[1] L. C. Andrews and R. L. Phillips, *Laser Beam Propagation through Random Media* (SPIE Optical Engineering Press, Bellingham, 1998).

[2] A. Ishimaru, *Wave Propagation and Scattering in Random Media* (IEEE Press, Piscataway, New Jersey, 1997); [previously published as Vols I & II by Academic, New York (1978)].

[3] W. B. Miller, J. C. Ricklin, and L. C. Andrews, "Effects of the refractive index spectral model on the irradiance variance of a Gaussian beam, J. Opt. Soc. Am. A **11**,2719-2726 (1994).

[4] W. B. Miller, J. C. Ricklin, and L. C. Andrews, "Scintillation of initially convergent Gaussian beams in the vicinity of the geometric focus," Appl. Opt. **34**, 7066-7073 (1995).

[5] M. S. Belen'kii and V. L. Mironov, "Mean diffracted rays of an optical beam in a turbulent medium," J. Opt. Soc. Am. **70**, 159-163 (1980).

[6] L. C. Andrews, W. B. Miller, and J. C. Ricklin, "Spatial coherence of a Gaussian beam in weak and strong optical turbulence," J. Opt. Soc. Am. A **11**, 1653-1660 (1994).

[7] C. Y. Young and L. C. Andrews, "Effects of a modified spectral model on the spatial coherence of a laser beam," *Waves Random Media* **4**, 385-397 (1994).

[8] J. C. Ricklin, W. B. Miller, and L. C. Andrews, "Effective beam parameters and the turbulent beam waist for initially convergent Gaussian beams," Appl. Opt. **34**, 7059-7065 (1995).

[9] L. C. Andrews, R. L. Phillips, C. Y. Hopen, and M. A. Al-Habash, "Theory of optical scintillation, J. Opt. Soc. Am. A **16**, 1417-1429 (1999).

[10] L. C. Andrews, R. L. Phillips, and C. Y. Hopen, "Aperture averaging of optical scintillations: power fluctuations and the temporal spectrum," Waves Random Media **10**, 53-70 (2000).

[11] A. Consortini, F. Cochetti, J. H. Churnside, and R. J. Hill, "Inner scale effect on intensity variance measured for weak to strong atmospheric scintillation," J. Opt. Soc. Am. A **10**, 2354-2362 (1993).

[12] A. Belmonte, "Feasibility study for the simulation of beam propagation: consideration of coherent lidar performance," Appl. Opt. **39**, 5428-5445 (2000).

[13] S. M. Flatté, C. Bracher, and G.-Yu Wang, "Probability-density functions of irradiance for waves in atmospheric turbulence calculated by numerical simulations," J. Opt. Soc. Am. A **11**, 2080-2092 (1994).

[14] L. C. Andrews, R. L. Phillips, C. Y. Hopen, and M. A. Al-Habash, "Theory of optical scintillation," J. Opt. Soc. Am. A **16**, 1417-1429 (1999).

[15] L. C. Andrews, R. L. Phillips, and C. Y. Hopen, "Aperture averaging of optical scintillations: power fluctuations and the temporal spectrum," Waves in Random Media **10**, 53-70 (2000)

[16] L. C. Andrews, R. L. Phillips, and C. Y. Hopen, "Scintillation model for a satellite communication link at large zenith angles," Opt. Eng. (To appear).

[17] R. J. Hill, R. G. Frehlich, and W. D. Otto, "The probability distribution of irradiance scintillation," NOAA Tech. Memo. ERL ETL-274 (NOAA Environmental Research Laboratories, Boulder, CO, 1996).

[18] R. J. Hill and R. G. Frehlich, "Probability distribution of irradiance for the onset of strong scintillation," J. Opt. Soc. Am. A **14**, 1530-1540 (1997).

[19] L. C. Andrews and R. L. Phillips, "*I-K* distribution as a universal propagation model of laser beams in atmospheric turbulence," J. Opt. Soc. Am. A **2**, 160–163 (1985).